

# PLANET FORMATION AROUND STARS OF VARIOUS MASSES: THE SNOW LINE AND THE FREQUENCY OF GIANT PLANETS

GRANT M. KENNEDY<sup>1</sup>

Research School of Astronomy and Astrophysics, Mt Stromlo Observatory, Australian National University, ACT 2611, Australia and  
ANU Planetary Science Institute, Australian National University, Canberra, Australia

AND

SCOTT J. KENYON

Smithsonian Astrophysical Observatory, Cambridge, MA 02138, USA

*Draft version May 31, 2018*

## ABSTRACT

We use a semi-analytic circumstellar disk model that considers movement of the snow line through evolution of accretion and the central star to investigate how gas giant frequency changes with stellar mass. The snow line distance changes weakly with stellar mass; thus giant planets form over a wide range of spectral types. The probability that a given star has at least one gas giant increases linearly with stellar mass from  $0.4 M_{\odot}$  to  $3 M_{\odot}$ . Stars more massive than  $3 M_{\odot}$  evolve quickly to the main-sequence, which pushes the snow line to 10–15 AU before protoplanets form and limits the range of disk masses that form giant planet cores. If the frequency of gas giants around solar-mass stars is 6%, we predict occurrence rates of 1% for  $0.4 M_{\odot}$  stars and 10% for  $1.5 M_{\odot}$  stars. This result is largely insensitive to our assumed model parameters. Finally, the movement of the snow line as stars  $\gtrsim 2.5 M_{\odot}$  move to the main-sequence may allow the ocean planets suggested by Léger et al. to form without migration.

*Subject headings:* planetary systems: formation — planetary systems: protoplanetary disks — stars: evolution — stars: formation

## 1. INTRODUCTION

In the last ten years, the discovery of more than 200 extra-solar planets,<sup>2</sup> and more than 200 debris disks,<sup>3</sup> suggests that planet formation is a common and robust process. Planet masses inferred from debris disks range from terrestrial to Jovian, at distances as great as tens of AU from the central star (e.g. Kenyon & Bromley 2004a; Greaves et al. 2005). The nature and sensitivity of radial velocity surveys means that most of the planets are  $\sim$ Jupiter mass gas giants in close orbits around Sun-like stars. However, recent discoveries as diverse as icy  $\sim$ Neptune-mass planets orbiting M dwarfs (e.g. Rivera et al. 2005), and debris disks around A-type stars (e.g. Rieke et al. 2005) show that planet formation occurs over a wide range of spectral types.

Current theory suggests that planets form in similar ways around all stars. Thus, the increasing diversity of stellar hosts and planetary systems provides an opportunity to test these theories. For this reason, the types of planets most likely to form around stars of differing spectral types has become a renewed area of study (e.g. Ida & Lin 2005; Boss 2006; Kornet et al. 2006; Kennedy et al. 2006), after the idea was first explored by Nakano nearly 20 years ago (Nakano 1987, 1988a,b).

Theories of Solar System formation generally include the “snow line,” where ices condense from the nebular

gas. The snow line distance is usually fixed in a disk with a time independent surface density and temperature profile around a main-sequence star (e.g. Ida & Lin 2005). In a more realistic picture, the disk and stellar properties evolve considerably during the 1–10 Myr pre-main-sequence (PMS) lifetime when planets probably form (e.g. Lissauer 1987; Pollack et al. 1996). As the disk temperature evolves with time, movement of the snow line may therefore influence the properties of theoretical planetary systems (e.g. Kennedy et al. 2006; Garaud & Lin 2007).

Here, we begin to develop a time dependent model for the formation of gas giant cores that considers the PMS evolution of the star and surrounding accretion disk. We introduce a simple semi-analytic disk model, based on the “minimum mass solar nebula,” that links movement of the snow line through evolution of disk accretion and stellar luminosity. In contrast to previous studies (e.g. Ida & Lin 2005; Kornet et al. 2006), our analysis suggests that gas giant formation around stars more massive than the sun is more likely than around less massive stars.

We cover the background important to our story in §2, consider the snow line in §3, and outline our model in §4. We present our results in §5, and discuss and conclude in §6 and §7.

## 2. BACKGROUND

Planetary systems form in circumstellar disks, which evolve on timescales comparable to the pre-main-sequence (PMS) stage of stellar evolution. Observations indicate a wide range of disk masses  $M_{disk} \sim 0.01\text{--}0.1 M_{\star}$  (where  $M_{\star}$  is the stellar mass, e.g. Osterloh & Beckwith 1995; Natta et al.

Electronic address: grant@mso.anu.edu.au

Electronic address: kenyon@cfa.harvard.edu

<sup>1</sup> *current address:* Smithsonian Astrophysical Observatory, Mail Stop 16, 60 Garden St, Cambridge, MA 02138, USA

<sup>2</sup> <http://vo.obspm.fr/exoplanetes/encyclo/encycl.html>

<sup>3</sup> <http://www.roe.ac.uk/ukatc/research/topics/dust/identification.htm>

2000; Andrews & Williams 2005; Eisner & Carpenter 2006; Scholz et al. 2006) and radii  $\sim 100\text{--}1000$  AU (McCaughrean & O’dell 1996). The lifetime of the primordial, optically thick, dusty component of the disk is  $\lesssim 10$  Myr, with a median timescale of  $\sim 3$  Myr (e.g. Strom et al. 1993; Haisch et al. 2001b). Though harder to observe, the gaseous component of the disk is probably removed by viscous accretion (Lynden-Bell & Pringle 1974) and photoevaporation (e.g. Hollenbach et al. 2000; Adams et al. 2004; Alexander et al. 2006) on similar timescales (Zuckerman et al. 1995; Pascucci et al. 2006).

These timescales place strict observational limits on the important stages of planet formation. Planetesimals must form rapidly to enable further grain growth and protoplanet formation by coagulation (e.g. Safronov 1969). To attract significant atmospheres and form gas giants, protoplanets need to reach masses of  $5\text{--}10 M_{\oplus}$  (e.g. Pollack et al. 1996; Ikoma et al. 2000) before the nebular gas is removed.

In coagulation models, dust particles on near circular orbits with small relative velocities grow through repeated collisions and mergers in circumstellar disks. Further dynamical evolution through “run-away” (Wetherill & Stewart 1989; Kokubo & Ida 1996) and “oligarchic” (Kokubo & Ida 1998) growth leads to “isolated” protoplanets, whose mass  $M_{iso}$  and spacing depend on their radial distance  $a$  from the central star via the Hill radius  $R_H = a(M_{iso}/3M_{\star})^{1/3}$  (e.g. Lissauer 1987; Lissauer & Stevenson 2007)

$$M_{iso} = \frac{(4\pi B\sigma a^2)^{3/2}}{(3M_{\star})^{1/2}}, \quad (1)$$

where  $\sigma$  is the disk surface density. Protoplanets are spaced at  $2BR_H \sim 8R_H$  intervals (Kokubo & Ida 1998). Used in combination with equation (1), the “minimum mass solar nebula” (MMSN, Weidenschilling 1977; Hayashi 1981) with  $\sigma \propto a^{-\delta}$  (where  $\delta = 1\text{--}1.5$ ), gives a simple model of protoplanet formation.

The “snow line”—the point in the disk that separates the inner region of rocky planet formation from the outer region of icy planet formation—is an important feature of the MMSN (e.g. Sasselov & Lecar 2000; Ida & Lin 2005; Ciesla & Cuzzi 2006). Condensation of ices outside the snow line increases the disk surface density by a factor  $f_{ice} \sim 3$ ,<sup>4</sup> which leads to factor of 5 larger isolation masses (eq. 1). In an MMSN model with  $\sigma = 10 \text{ g cm}^{-2}$  at 1 AU and  $\delta = 3/2$ ,  $M_{iso} \approx 0.1$  (1)  $M_{\oplus}$  at 1 (5) AU. To achieve the probable core mass of  $5\text{--}10 M_{\oplus}$  for Jupiter (Saumon & Guillot 2004) the MMSN can be augmented beyond the snow line by a factor  $\sim 4$ . Alternatively, if  $\delta = 1$  then  $M_{iso} \approx 5 M_{\oplus}$  at 5 AU. Models that relax the assumption of a smooth radial profile find an enhanced surface density near the snow line (e.g. Cuzzi & Zahnle 2004; Ciesla & Cuzzi 2006). A common theme among both MMSN and more detailed models is the surface density added by ice condensation.

Because the timescale for planet growth is  $t \propto P/\sigma \propto a^3$  for  $\sigma \propto a^{-3/2}$ , where  $P$  is the orbital period (e.g.

Lissauer 1987, see also Goldreich et al. (2004)), ice condensation also leads to shorter growth times. Numerical simulations by Kenyon & Bromley (2004a,b) find the time to form  $1000\text{--}3000$  km objects agrees with this relation. Numerical estimates of the time to form the Jovian core range from  $\sim 10^5\text{--}10^6$  yr (e.g. Lissauer 1987; Pollack et al. 1996; Inaba et al. 2003; Chambers 2006). In general, the time to reach isolation  $t_{iso}$  provides an estimate of whether protoplanets form early enough to accrete gas and become giant planets. Short gas disk lifetimes (e.g. Zuckerman et al. 1995; Pascucci et al. 2006), imply a relatively short isolation time, and place strong constraints on the time to form gas giants by core accretion.

Gas giant formation by core accretion occurs when protoplanet core masses are sufficient to attract gas from the nebula. The core mass sets the timescale for gas giant formation (Ikoma et al. 2000; Hubickyj et al. 2005). Cores with masses smaller than  $\sim 5 M_{\oplus}$  attract atmospheres (e.g. Inaba & Ikoma 2003), but are unable to form a gas giant before the nebular gas is removed on timescales of  $1\text{--}10$  Myr. Beyond the snow line the critical core mass where significant gas accretion occurs is  $M_{crit} \sim 7 M_{\oplus} \dot{M}_{core}^{0.25} \kappa^{0.25}$  (where  $\dot{M}_{core}$  is the rate at which planetesimals are accreted onto the core in units of  $10^{-7} M_{\oplus} \text{ yr}^{-1}$ , and  $\kappa$  is the grain opacity in units of  $\text{cm}^2 \text{ g}^{-1}$ , Ikoma et al. 2000, see also Rafikov (2006)). The critical core mass required to form Jupiter in several Myr ( $M_{iso} \sim 5\text{--}10 M_{\oplus}$ , Pollack et al. 1996; Hubickyj et al. 2005)—which implies  $\sigma \sim 10 \text{ g cm}^2$  at 5 AU—is consistent with the core mass inferred from current structural models (e.g. Saumon & Guillot 2004).

## 2.1. Previous Work

Most planet formation theories are based on a static MMSN disk around a solar-mass star. There are several motivating factors for extending these theories to a range of stellar masses: (i) the increasing stellar mass range of extra-solar planet hosts, (ii) observed trends with stellar mass, such as accretion rate and disk mass, and (iii) theoretical relations with variables that change with stellar mass, such as orbital period and isolation mass. This extension of Solar System theory to a range of spectral types began with a series of papers by Nakano nearly twenty years ago (Nakano 1987, 1988a,b). More recently, Kornet et al. (2006) considered formation of planets around stars of various masses *in situ*, while Ida & Lin (2005) examined observable planetary systems resulting from type II migration.

Kornet et al. consider disk evolution prior to the growth of large objects. In their models, the increased inward migration rate for planetesimals around low-mass stars results in higher absolute surface densities from  $0.1\text{--}100$  AU at 1 Myr. Thus low-mass stars are more likely to form giant planets. This result is influenced by their choice of an approximately constant initial disk mass for all stellar masses. They do not consider planet formation beyond 5 AU.

Ida & Lin base their Monte-Carlo study on the MMSN. Type II migration—where a planet with sufficient mass opens a gap in the disk and whose orbit is subsequently coupled to the viscous evolution of the disk (e.g. Lin & Papaloizou 1985)—is central to their model. In

<sup>4</sup> The usual value is  $\sim 4$ , but recent solar abundance figures for oxygen (Asplund et al. 2005) indicate 3 is more reasonable. Recent composition data from 9P/Tempel 1 may argue for an even lower ice/rock ratio (Küppers et al. 2005).

their attempt to reproduce the observed distribution of extra-solar planets, they find that close-in icy Neptune-mass planets should be much more common than close-in Jupiter-mass planets around M dwarf stars (see also Laughlin et al. 2004). In contrast to the Kornet et al. study, they find that the likelihood of a star harbouring gas giants increases with stellar mass up to solar-mass stars. Their results are influenced by scaling the snow line distance as  $a_{snow} \propto M_\star^2$ , based on the main-sequence luminosity  $L_\star \propto M_\star^4$ . As we show below, this simplification places the snow line too close to (far from) the central star for stars with masses less than (greater than) a Solar mass when protoplanets form.

In this paper we consider movement of the snow line as disk accretion subsides and the central star evolves to the main-sequence. Using our prescription for the snow line position over a range of stellar and disk masses, we locate regions where gas giant cores form. Assuming stars are born with disks from a distribution of masses, we then predict how gas giant frequency varies with stellar mass.

### 3. LOCATION OF THE SNOW LINE

In this section we consider evolution of the disk mid-plane temperature, and the snow line distance, with a simple model that includes accretion and PMS evolution. In particular, we are interested in the stellar mass dependence, rather than a detailed derivation for a single star. As we show in §5,  $\sim 1$  AU differences between our model and more detailed treatments (e.g. Sasselov & Lecar 2000; Lecar et al. 2006) do not affect our conclusions.

The disk mid-plane, where the gas density is highest, is probably where most ices condense, and has a temperature

$$T_{mid}^4 = T_{mid,accr}^4 + T_{irr}^4, \quad (2)$$

where  $T_{mid,accr}$  is the mid-plane temperature arising from viscous forces within the disk, and  $T_{irr}$  is temperature due to external irradiation of the disk by the central star.

The effective disk temperature from viscous accretion is (Lynden-Bell & Pringle 1974)

$$T_{eff,accr}^4 = \frac{3}{8\pi} \frac{GM_\star \dot{M}}{\sigma_{sb} a^3} \left(1 - \sqrt{\frac{R_\star}{a}}\right), \quad (3)$$

where  $\dot{M}$  is the accretion rate,  $R_\star$  is the stellar radius, and  $\sigma_{sb}$  is Stefan’s constant. In optically thick regions near the snow line, the mid-plane temperature is  $T_{mid,accr}^4 \sim 3\tau T_{eff,accr}^4/8$  (Hubeny 1990), where  $\tau = \kappa\sigma_g/2$ . The opacity  $\kappa$  is a function of temperature (Bell & Lin 1994), and the gas surface density  $\sigma_g$  is 100 times greater than that of solids. The figure of 100 is used in converting mm dust observations to total disk masses (e.g. Natta et al. 2000) based on the interstellar gas/dust ratio, and is similar to the solar metallicity (Z) fraction of 0.0122 (Asplund et al. 2005). The accretion rate varies with stellar mass as approximately  $\dot{M} \propto M_\star$  for the range of stellar masses we consider (0.2–4  $M_\star$ , Muzerolle et al. 2003), and with time as  $\dot{M} \propto (t/10^6 \text{ yr})^{-\gamma}$ . Hartmann et al. (1998) derive  $\gamma = 1.5$ –2.8. The uncertainty is due to the limited age range of their sample and a large range of accretion rates

at a given age. The value  $\gamma = 1.5$  is their “preferred result.” We scale  $\dot{M}$  with surface density, which accounts for the observed trend with stellar mass (if disk mass scales linearly with stellar mass, see §4), and is consistent with expected viscous evolution (where  $\dot{M} \propto \nu\sigma$  and  $\nu$  is the disk viscosity). For  $\sim 1$  Myr old Solar-type stars  $\dot{M} \sim 10^{-8} M_\odot \text{ yr}^{-1}$  (Hartmann et al. 1998). We set  $\dot{M} = 10^{-8} M_\odot \text{ yr}^{-1}$  for an initially three-fold enhanced MMSN disk, as this disk decays to the “typical” observed  $\sim$ MMSN mass disk by  $\sim 1$  Myr (Hartmann et al. 1998).

A more complete treatment of the optical depth to the mid-plane would include evolution of the gas surface density, allowing the mid-plane temperature to drop somewhat faster than described above as  $\sigma_g$  decreases in the inner disk (Lynden-Bell & Pringle 1974). The solid surface density, which largely resides near the mid-plane and determines protoplanet characteristics, remains largely unaffected by the gas disk evolution (aside from snow line evolution).

The disk temperature contribution from irradiation is

$$T_{irr} = T_\star \left(\frac{\alpha}{2}\right)^{1/4} \left(\frac{R_\star}{a}\right)^{3/4}, \quad (4)$$

where  $\alpha \approx 0.005/a_{AU} + 0.05a_{AU}^{2/7}$  for a flared disk in vertical hydrostatic equilibrium (e.g. Adams & Shu 1986; Kenyon & Hartmann 1987; Chiang & Goldreich 1997). Here  $a_{AU}$  is  $a$  in units of AU. When the disk is optically thick to radiation at this temperature,  $T_{irr}$  is approximately the interior temperature for a flared disk (Chiang & Goldreich 1997).

Figure 1 shows the location of the snow line in disks with  $\sigma = \sigma_{MMSN} M_\star/M_\odot$  for several different stellar masses over time for irradiation only, and for accretion + irradiation. We locate the snow line where  $T_{mid} = 170$  K. More detailed derivations of this temperature (e.g. Podolak & Zucker 2004; Lecar et al. 2006) do not change the snow line distance significantly. For PMS stellar properties we use Palla & Stahler (1999) tracks. For comparison, we also show the (fixed) snow line distance for stars on the main-sequence (e.g. Ida & Lin 2005).

Looking first at the Solar case, the snow line moves inward over time. This movement is always determined by viscous accretion, and its decay over time. Our snow line crosses the “canonical” distance of 2.7 AU at  $5 \times 10^5$  yr. For disks with accretion rates so low that irradiation dominates, the snow line still moves inward over time, as illustrated by the dashed line for  $T_{irr}$ .

For more massive stars,  $T_{irr}$  begins to dominate as accretion subsides and the star quickly evolves to a significantly greater main-sequence luminosity. Irradiation becomes important at a few Myr for 2  $M_\odot$  stars, and  $\sim 1$  Myr for 3  $M_\odot$  stars. The large discrepancy between our snow line, and that of Ida & Lin (2005) (who considered  $0.2 M_\odot < M_\star < 1.5 M_\odot$ ) arises because theirs is based on the main-sequence luminosity ( $L_\star \propto M_\star^4$ ) and an optically thin disk ( $T_{disk}^4 \propto L_\star a^{-2}$ ). With our model, the snow line distance is less sensitive to stellar mass, allowing icy protoplanet formation relatively close ( $\sim 5$ –10 AU) to the central star for intermediate mass stars. At these closer distances, the surface density is higher and formation is faster, making it more likely that protoplanets massive enough to undergo core accretion will

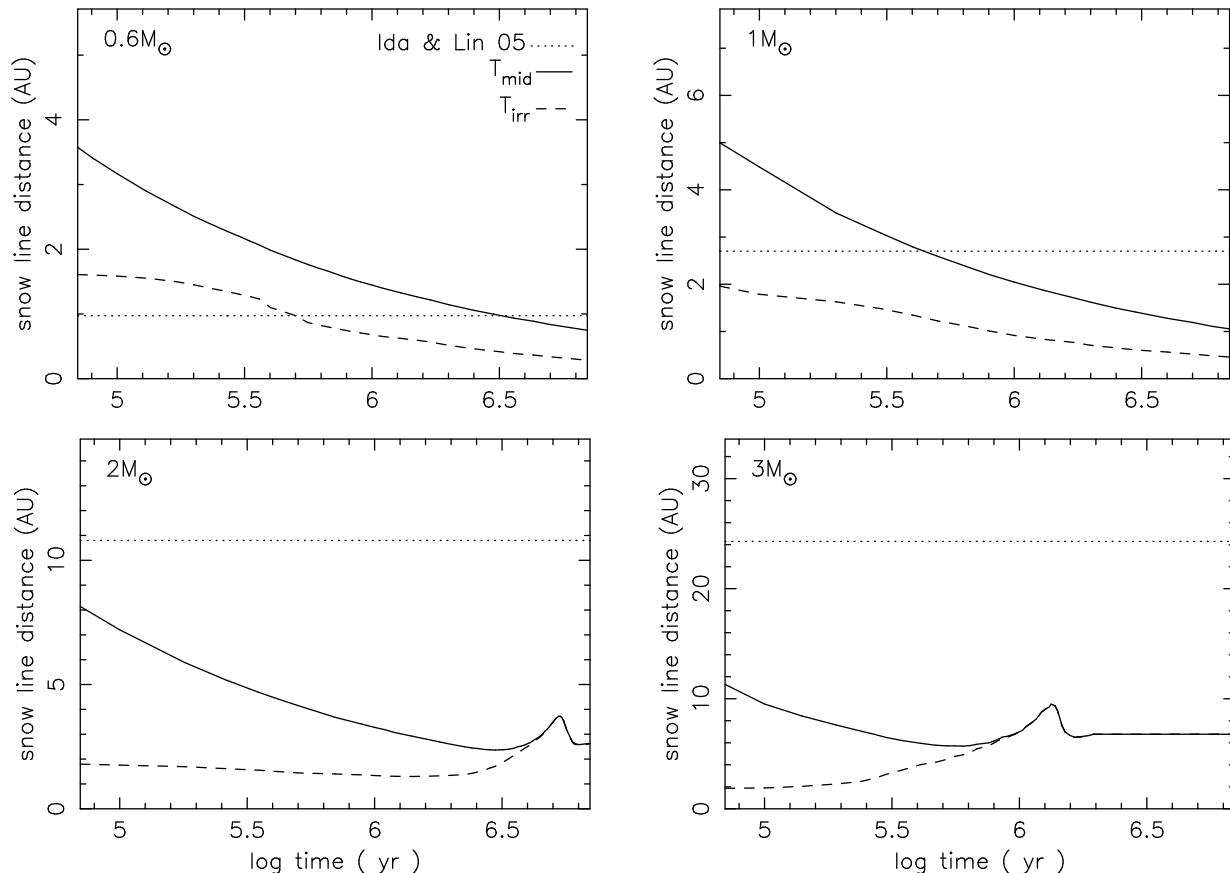


FIG. 1.— Location of the snow line ( $a$  at  $T_{mid} = 170$  K) over time for 0.6, 1, 2, and  $3 M_{\odot}$  stars (left to right, and down) with irradiation only (using Palla & Stahler (1999) PMS tracks, dashed line), and irradiation + accretion (solid line). The disks have surface densities  $\sigma = \sigma_{\text{MMSN}} M_{\star}/M_{\odot}$ . Included for reference is  $a_{\text{snow}} = 2.7 M_{\star}/M_{\odot}$  AU as used by Ida & Lin (2005) (dotted line).

form. For less massive stars, the snow line is still at a few AU, where isolation times are relatively long, making it difficult to form cores before the gas disk is dissipated. Comparison of the snow line distance with typical disk lifetimes of several Myr leads to an increasing snow line distance with stellar mass.

With the snow line evolution established, we now describe our model of protoplanet formation.

#### 4. PROTOPLANET FORMATION MODEL

The MMSN is a simple model disk for the origin of the Solar System, and has  $\sigma(a) = \sigma_0 f_{ice} a^{-\delta}$ , where the factor  $f_{ice}$  represents a jump in surface density at the snow line distance  $a_{\text{snow}}$ , and  $\delta$  is usually 3/2. To extend this model to a range of stellar masses requires consideration of how disk mass varies with stellar mass. Observations indicate  $M_{\text{disk}} \propto M_{\star}$  (Natta et al. 2000; Scholz et al. 2006); however, there is a wide range of disk masses at any given stellar mass. Thus, to extend the MMSN model to a range of stellar and disk masses, we adopt the surface density relation

$$\sigma(a, t) = \sigma_0 \eta f_{ice} \frac{M_{\star}}{M_{\odot}} a_{\text{AU}}^{-\delta}, \quad (5)$$

where  $\sigma_0 = 10 \text{ g cm}^{-2}$ . The factor  $\eta$  changes the disk mass relative to the star (“relative disk mass”), and is varied to account for the observed range of disk masses at fixed stellar mass. Current observations suggest  $\eta \sim 0.5$ – $5$  ( $M_{\text{disk}} = 0.01$ – $0.1 M_{\star}$ );  $\eta \sim 10$  is the upper limit for

disk stability ( $M_{\text{disk}} \sim 0.25 M_{\star}$ ). To provide a smooth transition from  $f_{ice} = 1$  for  $a \lesssim a_{\text{snow}}$  to  $f_{ice} = 3$  for  $a \gtrsim a_{\text{snow}}$ , we set  $f_{ice} = 1 + (\Delta_{ice} - 1)/(1 + e^x)$  where  $\Delta_{ice} = 3$ ,  $x = (a_{\text{snow}} - a)/\Delta a_{\text{snow}}$  and  $\Delta a_{\text{snow}}$  is the radial distance equivalent to a 5 K temperature change.

Combined with the local orbital period, the surface density sets the time to form protoplanets, and sets whether protoplanets form early enough to accrete gas and become gas giants. We introduce a stellar mass dependence, so our isolation timescale, based on numerical simulations by Kenyon & Bromley (2004a,b), becomes

$$t_{iso} \propto (\eta\sigma)^{-1} a^{3/2} M_{\star}^{-1/2}. \quad (6)$$

The normalisation of equation (6) depends on the size of the small objects (e.g. Goldreich et al. 2004; Chambers 2006). We use  $10^5 \text{ yr}$  for  $\sigma = 10 \text{ g cm}^{-2}$  at 5 AU, based on the likelihood of small fragmented bodies to accrete (e.g. Kenyon & Bromley 2004a), and the consequent short growth times (Rafikov 2004; Chambers 2006). Hubickyj et al. (2005) infer  $t_{iso} \lesssim 5 \times 10^5 \text{ yr}$  for much larger 100 km planetesimals. As long as the Jovian timescale is somewhat shorter than the gas disk lifetime, this choice affects our results little.

Under the assumption that stars all form disks in  $\sim 10^5 \text{ yr}$  (based on an infall rate of  $10^{-5} M_{\odot} \text{ yr}^{-1}$ , Palla & Stahler 1999), and that planetesimal formation is relatively fast (Weidenschilling 2000; Dullemond & Dominik 2005), we add a constant offset of  $10^5 \text{ yr}$  to the isolation timescale to reconcile the tim-

ing of isolation with disk and stellar evolution. Though this time is uncertain, removing or moderately modifying the offset does not affect our results significantly because  $t_{iso}$  is usually  $\gtrsim 10^5$  yr.

We adopt a range of disk masses, integrated from the inner disk radius to 60 AU, with a gas to solids ratio of 100. For  $\delta = 3/2$ ,  $\eta = 4$  corresponds to a relatively massive disk  $M_{disk} = 0.1 M_*$ . This enhancement is our baseline model and yields the surface density and core mass needed to form Jupiter on reasonable time scales (Pollack et al. 1996; Ikoma et al. 2000). For  $\delta = 1$ , smaller  $\eta$  yields the same disk mass because more mass is placed at larger radii. For  $\eta = 1$  and  $\delta = 1$ ,  $M_{disk} = 0.12 M_*$ .

### 5. REGIONS THAT FORM GAS GIANT CORES

The successful formation of a gas giant planet by core accretion requires satisfaction of two main conditions. A core must form while the gaseous component of the circumstellar disk is still present, and it must be massive enough to attract a large atmosphere before this gas is dispersed. Prior to isolation, accreted planetesimals and a sub-critical protoplanet mass limit gas accretion. After isolation, if a protoplanet is massive enough, and forms while the gas disk is still present, significant gas accretion proceeds. This separation into two classes, gas giants and “failed cores,” reflects the expected paucity of 20–100  $M_{\oplus}$  planets over a range of stellar masses (Ida & Lin 2005).

To form a gas giant in less than  $10^7$  yr, various studies suggest a minimum core mass of 5–10  $M_{\oplus}$  (Ikoma et al. 2000; Inaba et al. 2003; Hubickyj et al. 2005). Although the core mass depends on the planetesimal accretion rate and the opacity, the derived sensitivity is weak ( $M_{core} \propto \dot{M}^{0.25}$ ; Ikoma et al. 2000, see also Rafikov (2006)). A limited reservoir of planetesimals to accrete after isolation means high accretion rates cannot be sustained (and  $\dot{M}$  will decrease), while low accretion rates lower  $M_{core}$ . Thus, we adopt a minimum core mass  $M_{core} = 10 M_{\oplus}$  as a baseline, and consider  $M_{core} = 5 M_{\oplus}$  in §5.4.

The timescale for gas dissipation sets our second restriction. The gaseous component of the disk disperses in  $\lesssim 10$  Myr (Zuckerman et al. 1995; Pascucci et al. 2006). With  $\dot{M} \propto \sigma$ , the dissipation timescale for a viscous disk  $t_d \propto M_{disk}/\dot{M} \sim \text{constant}$  for our assumptions. Because the disk mass decreases significantly ( $\sim 60\%$ ) in 1 Myr, we adopt  $t_{core} = 1$  Myr as a typical maximum core formation time for all disks. Henceforth we reserve the word “core” for a protoplanet with  $M_{iso} > M_{core}$  and  $t_{iso} < t_{core}$ . Relatively little is known about the evolution of the gaseous component of the disk; we comment further on the consequences of varying  $t_{core}$  and other parameters in §5.4.

To investigate locations within circumstellar disks where gas giant cores form, we first derive results for a  $1 M_{\odot}$  star, and then consider a range of stellar masses. We restrict our study to stars with masses  $0.2$ – $4 M_{\odot}$ . For stars with masses  $< 0.2 M_{\odot}$  our model does not form gas giants. The short main-sequence lifetime of massive stars ( $M_* > 4 M_{\odot}$ ) makes them much less likely targets for planet detection. Some oligarchs do not reach masses sufficient for core accretion. Those cores that do form compete with other cores for dynamical space in

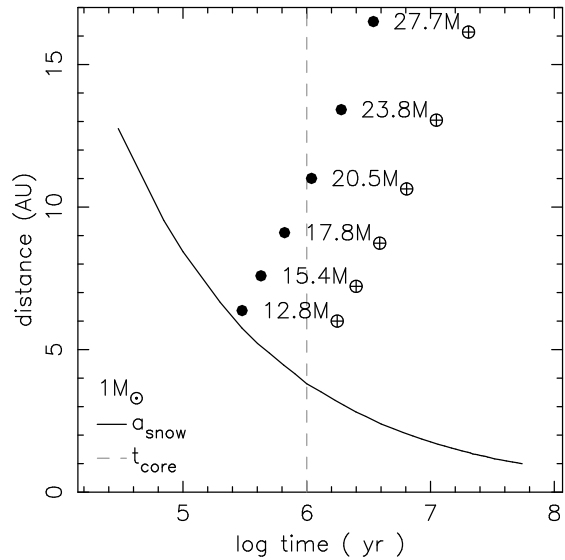


FIG. 2.— Isolation mass (filled circles, labelled with  $M_{iso}$ ) as a function of radial distance and PMS model time, for a solar mass star with the MMSN model with  $\eta = 4$  and  $\delta = 3/2$ . Masses are spaced at  $8 R_H$  intervals and only shown outside the snow line. The solid line shows  $a_{snow}$  over time, and the dashed vertical line is the time  $t_{core} = 1$  Myr.

the disk. We defer consideration of these objects to §5.3.

#### 5.1. The Solar Example

In this subsection we show how the MMSN disk model, the moving snow line, and the isolation mass and time combine to give a picture of the Solar System structure at  $\sim 1$  Myr.

Figure 2 shows isolation masses for the MMSN model beyond the snow line with  $\eta = 4$ , as a function of time and radial distance from the Sun. The isolation mass and timescale are calculated from the equations described in §4. Accretion and PMS tracks from Palla & Stahler (1999) set  $a_{snow}$  as described in §3.

When the first objects reach isolation, the Sun is in the early stages of its PMS contraction, and the accretion rate is  $\sim 10^{-7} M_{\odot} \text{ yr}^{-1}$ . Consequently the snow line is at  $\sim 6$  AU, which determines where the innermost icy protoplanet forms. This protoplanet is massive enough to become a gas giant (a core), so we refer to this position as the inner edge of the core-forming region. In the absence of significant migration from disk interaction, this result may help explain why Jupiter is at 5 AU. As the Sun continues to contract and accretion decreases, isolation is reached at ever increasing distances beyond the snow line. Eventually, the isolation time becomes longer than  $t_{core}$ , and protoplanets form too late to undergo core accretion. Isolation masses increase with distance from the Sun, so  $t_{core}$  always sets the outer edge of the core-forming region, and the number of cores that form. If the cores are spaced by  $8 R_H$  at isolation (as in Figure 2), then  $\sim 4$  cores form in this region and the region extends from  $\sim 6$ – $11$  AU, similar to the region containing Jupiter and Saturn today.

#### 5.2. A Range of Stellar Masses

We now consider how the core-forming region for a solar mass star changes with stellar mass between  $0.2 M_{\odot}$  and  $4 M_{\odot}$ . The processes described in §5.1 still apply,

but differences arise due to the linear relation between disk surface density and stellar mass, the different orbital periods around other stars, and the changing snow line distance due to the evolution of accretion and the central star.

Figure 3 shows isolation masses for 0.6 and  $3 M_{\odot}$  stars, with  $t_{core} = 1$  Myr and the same relative disk mass as Figure 2. The lower mass star does not form any cores, as the first object with  $M_{iso} > M_{core}$  forms after  $t_{core}$ . However, large 5–10  $M_{\oplus}$  objects still form (see §5.3.1). A longer  $t_{core}$  allows some of these to become cores, so whether lower mass stars form gas giants is sensitive to both  $M_{core}$  and  $t_{core}$ .

The  $3 M_{\odot}$  star forms its innermost core just inside the snow line at  $\sim 8$  AU, and the outermost is at  $\sim 20$  AU. Cores can form before  $t_{core}$  at greater distances due to decreased  $P$  and increased  $\sigma$ . The greater surface density in disks around these stars allows rocky cores to form interior to the snow line (see also Ida & Lin 2005). The large mass of the cores ( $\gg M_{core}$ ) in these relatively massive disks probably allows some gas accretion prior to isolation, which requires a numerical model of growth for more investigation (see also §5.4).

The results over a range of stellar masses can be combined into a single figure that considers the core-forming regions as a function of stellar mass. Figure 4 shows the core-forming region as a function of radial distance and stellar mass for our model, with standard parameters of  $t_{core} = 1$  Myr,  $M_{core} = 10 M_{\oplus}$ , and  $\delta = 3/2$ . Each contour represents the inner, outer, and stellar mass limits for forming cores with a particular relative disk mass. On the  $\eta = 4$  contour (outlined in the figure), the 6–10 AU range from Figure 2 contributes the points  $y = 6$  AU and  $y = 10$  AU for  $x = 1 M_{\odot}$ . Similarly, the 8–20 AU range from the right panel of Figure 3 contributes points at  $x = 3 M_{\odot}$ .

In general, Figure 4 shows that as stellar mass increases, disks with lower relative disk masses form cores, and the width of the regions where these cores form increases. Stars more massive than  $\sim 1.2 M_{\odot}$  form rocky cores interior to the snow line for relatively high disk masses. The core-forming region expands outward with increasing relative disk mass because the isolation timescale becomes shorter. Doubling the disk mass allows  $a$  to increase by a factor of  $\sim 1.6$  to keep the same  $t_{iso}$  (eq. 6).

As stellar mass increases, cores form in disks with decreasing relative disk mass. As  $\eta$  decreases, the inner edge of the core-forming region moves inward, because the accretion rate is lower and the disk has lower optical depth (so the mid-plane is cooler), and the snow line has evolved closer to the star by the time isolation is reached. The snow line is roughly the lower edge of the darker (lower  $\eta$ ) contours.

If  $M_{iso}$  does not jump to a value  $> M_{core}$  due to  $f_{ice}$  at the snow line, a core still forms further out. Thus, the inner edge moves to greater distances as the stellar mass—and hence absolute disk mass—decreases for fixed relative disk mass. However, the  $t_{core}$  restriction means that oligarchs around sufficiently low-mass stars do not reach isolation in time, and that all contours have a lower stellar mass limit.

The lowest disk mass that forms cores has  $\eta = 1.2$ , and only does so for  $3 M_{\odot}$ . For more massive stars, irradi-

ation overcomes accretion as the star reaches the main-sequence, and the larger snow line distance makes formation of cores more difficult (see also Ida & Lin 2005). Thus  $3 M_{\odot}$  stars are the most likely to form at least one gas giant, as they form cores over the widest range of disk masses.

The width of the regions where cores form increases with stellar mass (Figure 4, Ida & Lin 2005). The spacing of cores remains roughly constant with different stellar mass ( $M_{iso} \propto \sigma^{3/2}/\sqrt{M_{\star}} \propto M_{\star}$  and  $R_H \propto (M_{iso}/M_{\star})^{1/3}$  for  $\delta = 3/2$ , see also Figs. 2 & 3). However, the number of cores is not linearly related to the region width, since the spacing becomes wider with increasing distance. The width of the regions depends strongly on disk mass, particularly for disks that form cores interior to the snow line. The increasing width of the core-forming regions suggests that the number of cores (and therefore planets) in individual planetary systems increases with stellar mass.

To summarise, the range of relative disk masses that form gas giant cores increases with stellar mass, as does the width of the regions they form in. The first result leads to the expectation that the likelihood of forming gas giants increases with stellar mass. We make a quantitative prediction in §6.1.

While the core-forming regions are our primary interest, there are large regions of parameter space where oligarchs are relatively massive, but will not form gas giants. We consider these planets now.

### 5.3. Other Planets

The discovery of exoplanets with masses smaller than Neptune suggests that planet formation might often yield failed cores—oligarchs that did not accrete gas from the disk. Neptune and Uranus may be considered failed cores. Several theoretical studies (e.g. Laughlin et al. 2004; Ida & Lin 2005, this paper) suggest that failed cores are more common around low mass stars.

#### 5.3.1. Failed Cores

In our model, there are three ways to produce failed cores. Objects that form too late ( $t_{iso} > t_{core}$ ), or form with insufficient mass to accrete gas ( $M_{iso} < M_{core}$ ) are failed cores. Although all cores within the core-forming region can potentially accrete gas, dynamical interactions among the cores may eject one or more into regions with a small gas surface density (e.g. Thommes et al. 1999) or from the system entirely (e.g. Goldreich et al. 2004; Ford & Chiang 2007). This mechanism occurs in a random (and currently unquantifiable) fraction of models with  $M_{iso} > M_{core}$  and  $t_{iso} < t_{core}$ . In our model failed cores are more common around low-mass stars because isolation masses are smaller, and isolation times are longer.

Apparent failed cores may also form by collisions over long timescales (Kennedy et al. 2006). The mass of these icy planets may be limited by the likelihood of collisions vs. ejections during the final stages of coalescence (Goldreich et al. 2004).

#### 5.3.2. Ocean Planets

The diversity of observed extra-solar planets led Léger et al. (2004) to suggest that 1–10  $M_{\oplus}$  icy planets

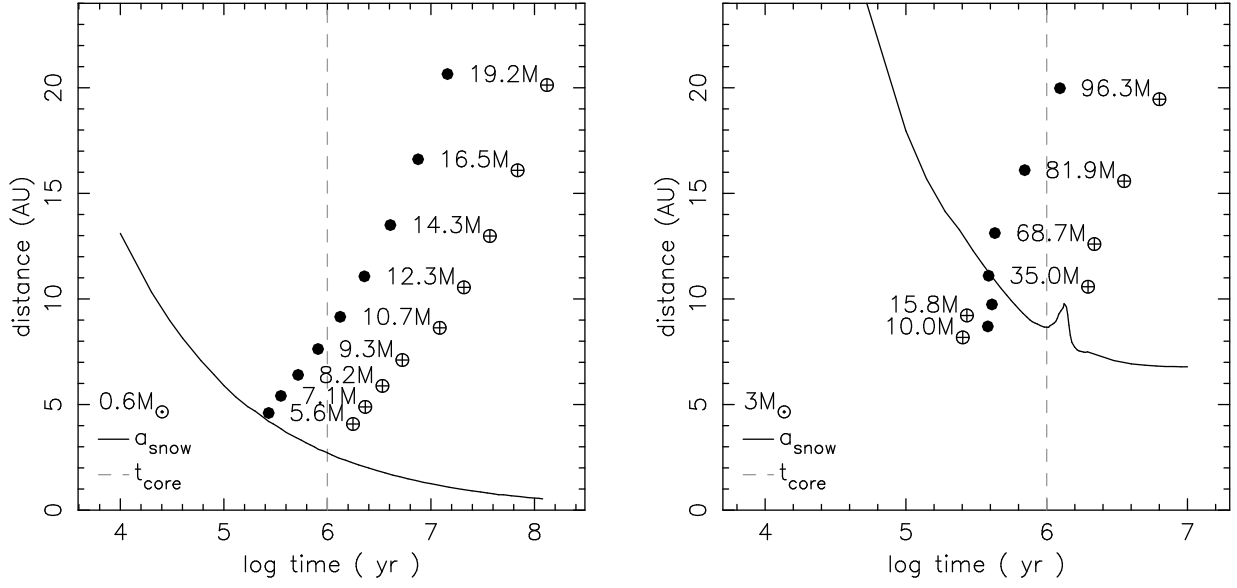


FIG. 3.— Same as Figure 2, but for  $0.6 M_{\odot}$  (left) and  $3 M_{\odot}$  (right). Isolation masses are only plotted outside the snow line, or where  $M_{\text{iso}} > M_{\text{core}}$ .

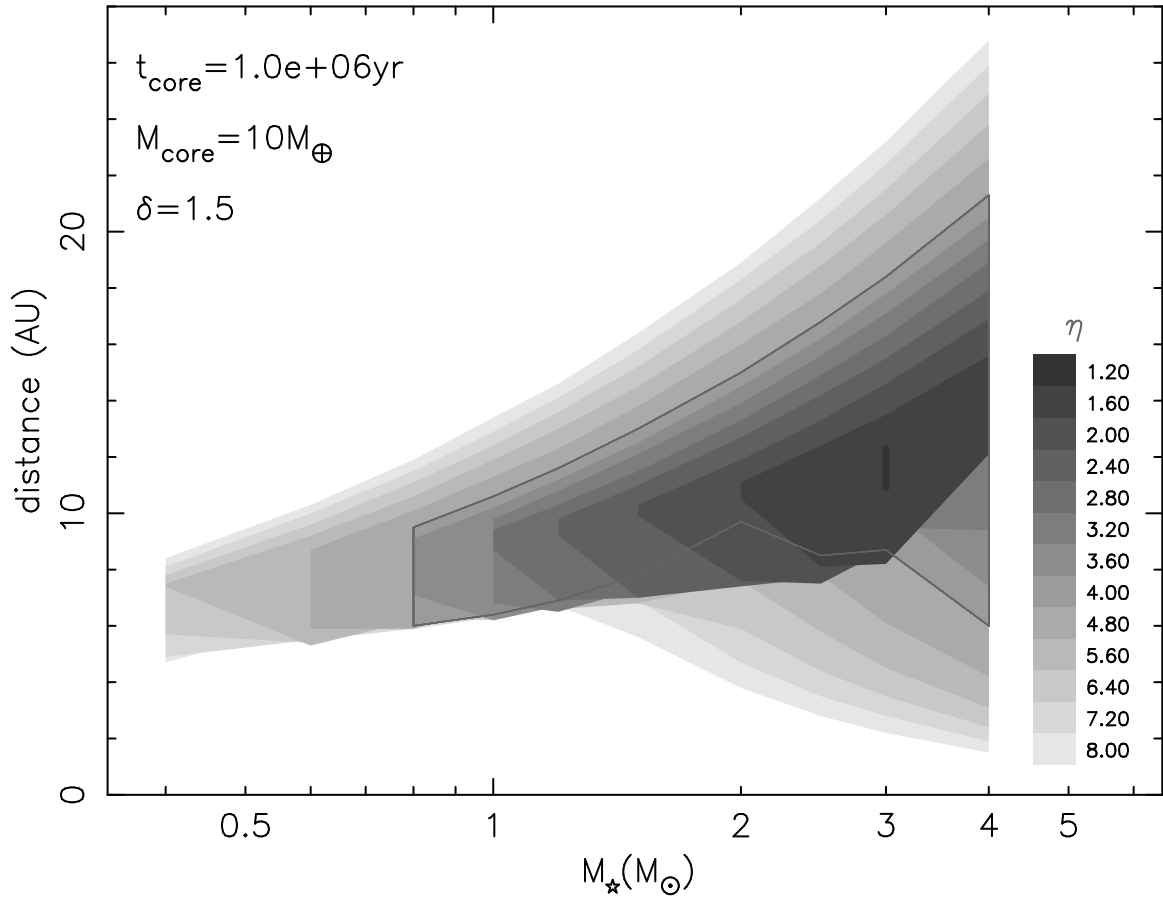


FIG. 4.— Regions where  $10 M_{\oplus}$  cores form in  $\leq 10^6$  yr as a function of radial distance and stellar mass. Each contour represents the inner, outer, and stellar mass limits for a particular  $\eta$  (and corresponding  $M_{\text{disk}}$ ), as shown by the legend. Our baseline model,  $\eta = 4$  is outlined. For  $\eta = 1.2$ , only  $3 M_{\odot}$  stars form cores.

that form in the region beyond the snow line may migrate inward to  $\sim 1$  AU, where the outer layers subsequently “melt.” With masses too low to accrete much gas, these planets are less dense than a rocky planet of equivalent mass and harbour deep oceans. Hence Léger et al. call these “ocean planets.”

The increase in luminosity of stars with masses  $\gtrsim 2.5 M_\odot$  as they reach the main-sequence provides an alternative *in situ* formation mechanism for ocean planets, as they may have insufficient mass for significant migration. We outline the concept briefly, because these planets are difficult to detect. At times  $\gtrsim 1$ – $10$  Myr, the snow line moves to  $\sim 10$  AU as the disk becomes optically thin.<sup>5</sup> Failed cores in the range  $1$ – $10 M_\oplus$  can therefore achieve their final mass outside the snow line in  $\sim 1$  Myr, and without migrating, later find themselves in a much warmer region when the star reaches the main-sequence.

Though all stars more massive than the Sun undergo an increase in luminosity as they settle onto the main-sequence (e.g. Palla & Stahler 1999), the temperature at the early snow line distance of  $\sim 7$  AU must increase enough to melt ice and maintain oceans. For  $2.5 M_\odot$ , there is  $\sim 1$  AU overlap between the early snow line, and the final habitable zone distance—at an equilibrium temperature of  $\sim 245$  K (Kasting et al. 1993)—with room for a few cores that form *in situ* just beyond the snow line.

#### 5.4. Sensitivity to Model Assumptions

Our model is simplified, but captures some important concepts. In this section, we show that our results remain for realistic variations on our model assumptions.

We use a simple model for the temperature profile of an irradiated, accreting, flared disk, which sets the location of the snow line. As shown in Figure 4,  $\sim 1$  AU changes in the snow line distance affects where the innermost cores originate, but there is little change in the range of disk masses that forms massive cores for a given stellar mass.

The disk surface density profile is uncertain: the MMSN assumes the Solar System planets formed *in situ*. In the standard MMSN model,  $\delta = 3/2$  and  $\eta = 4$  yield the surface density needed to form a massive core near Jupiter. If  $\delta = 1$  and  $\eta = 1$ , then  $M_{iso} \approx 5$  ( $13$ )  $M_\oplus$  at  $5$  ( $10$ ) AU, which are similar to the inferred core masses for Jupiter and Saturn (Saumon & Guillot 2004). Figure 5 shows the core-forming regions for  $\eta = 1$ ,  $\delta = 1$  and  $M_{core} = 5 M_\oplus$ . The lower  $\sigma$  in the core-forming regions needed to keep the same disk mass makes it harder to form cores with  $M_{core} = 10 M_\oplus$ , but with  $M_{core} = 5 M_\oplus$  the regions are similar to our baseline model.

There is little observational constraint of gaseous inner disk lifetimes, so the least certain of the parameters we specify is  $t_{core}$ . The isolation time is  $t_{iso} \propto a^3$  (when  $\delta = 3/2$ ), so doubling  $t_{core}$  allows the outer edge to move outward by a factor of about 1.3. Figure 6 shows how changing  $t_{core}$  alters the core-forming region with  $\eta = 4$  for  $M_{core} = 5 M_\oplus$  and  $10 M_\oplus$ , and  $\delta = 1$  and  $3/2$ . Longer gaseous disk lifetimes lead to more gas giant cores. The general trend is to extend the regions to lower stellar masses and to greater radial distances. Cores that take longer to form—due to smaller  $P$  or  $\sigma$ —can reach isola-

<sup>5</sup> The snow line has less meaning at these times, since there is little gas to condense into ices. The equilibrium temperature of objects is a more relevant concept.

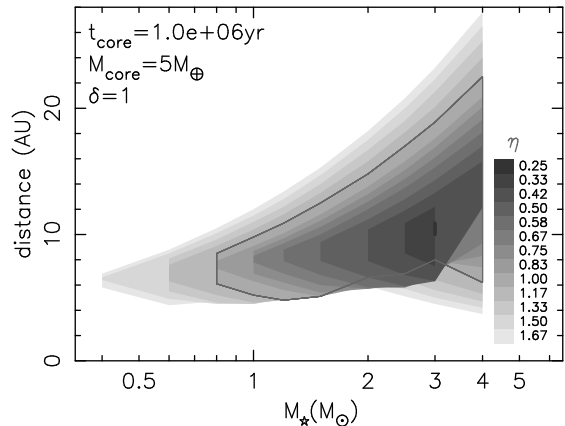


FIG. 5.— Same as Figure 4, but for  $\delta = 1$  and  $M_{core} = 5 M_\oplus$ . For  $\eta = 0.25$ , only  $3 M_\odot$  stars form cores. Though the  $\delta = 1$  disk has different  $\eta$ , it covers the same range of disk masses as Figure 4 with  $\delta = 3/2$ , with the exception of the lowest disk mass ( $\eta = 1.2$ ) from that figure.

tion before the gas disk is dissipated.

Dust disks around spectral types earlier than  $\sim G$  have somewhat shorter lifetimes than disks around lower mass stars (Haisch et al. 2001a; Currie et al. 2007). If gas is removed on timescales similar to infra-red excesses for a range of spectral types,  $t_{core}$  is shorter and the outer edge of the core-forming region for these stars moves in (Fig. 6). Observations of evolved stars can test whether a strongly stellar mass dependent  $t_{core}$  (or some other process) defines an upper stellar mass limit for gas giant formation.

The short timescale for disk removal by the central star—inferred from the lack of transition disks (e.g. Kenyon & Hartmann 1995; Clarke et al. 2001; Alexander et al. 2006)—and the likely large radial distance in the disk for external influence by massive stars (Adams et al. 2004), supports our assumption that the location of photoevaporation is unimportant. Although the expected distance for external photoevaporation in “typical” clusters reaches closer to the central star for low-mass stars (Adams et al. 2004), it lies outside the core-forming region for our standard case of  $M_{core} = 10 M_\oplus$ ,  $t_{core} = 10^6$  yr, and  $\delta = 1.5$ . The core-forming and external photoevaporation regions begin to overlap for  $M_\star \lesssim 0.5 M_\odot$  and  $t_{core} \gtrsim 5 \times 10^6$  yr.

The size of planetesimals is uncertain, as is the isolation time that results from their accretion by oligarchs. Our choice of  $10^5$  yr for the Jovian core is relatively short, and is based on likely fragmentation (e.g. Kenyon & Bromley 2004a) and the rapid accretion of small  $\sim 100$  m planetesimals in the shear dominated regime (e.g. Rafikov 2004; Chambers 2006). If planetesimals are larger and  $t_{iso}$  is longer (e.g. 1 Myr), similar results can be obtained by simply using a longer (yet still reasonable)  $t_{core} \sim 3$  Myr.

Choosing  $M_{core} = 5 M_\oplus$  allows core formation in less massive disks. Halving  $M_{core}$  allows a disk 1.6 times ( $M_{iso} \propto \sigma^{3/2}$ ) less massive to form cores in the same region, and also extends the region to lower stellar masses (Fig. 6).

We have chosen to ignore type I migration, where linear theory predicts that protoplanets excite spiral density waves in the gas disk, and migrate toward the central star on  $0.01$ – $0.1$  Myr timescales (Tanaka et al. 2002). Recent

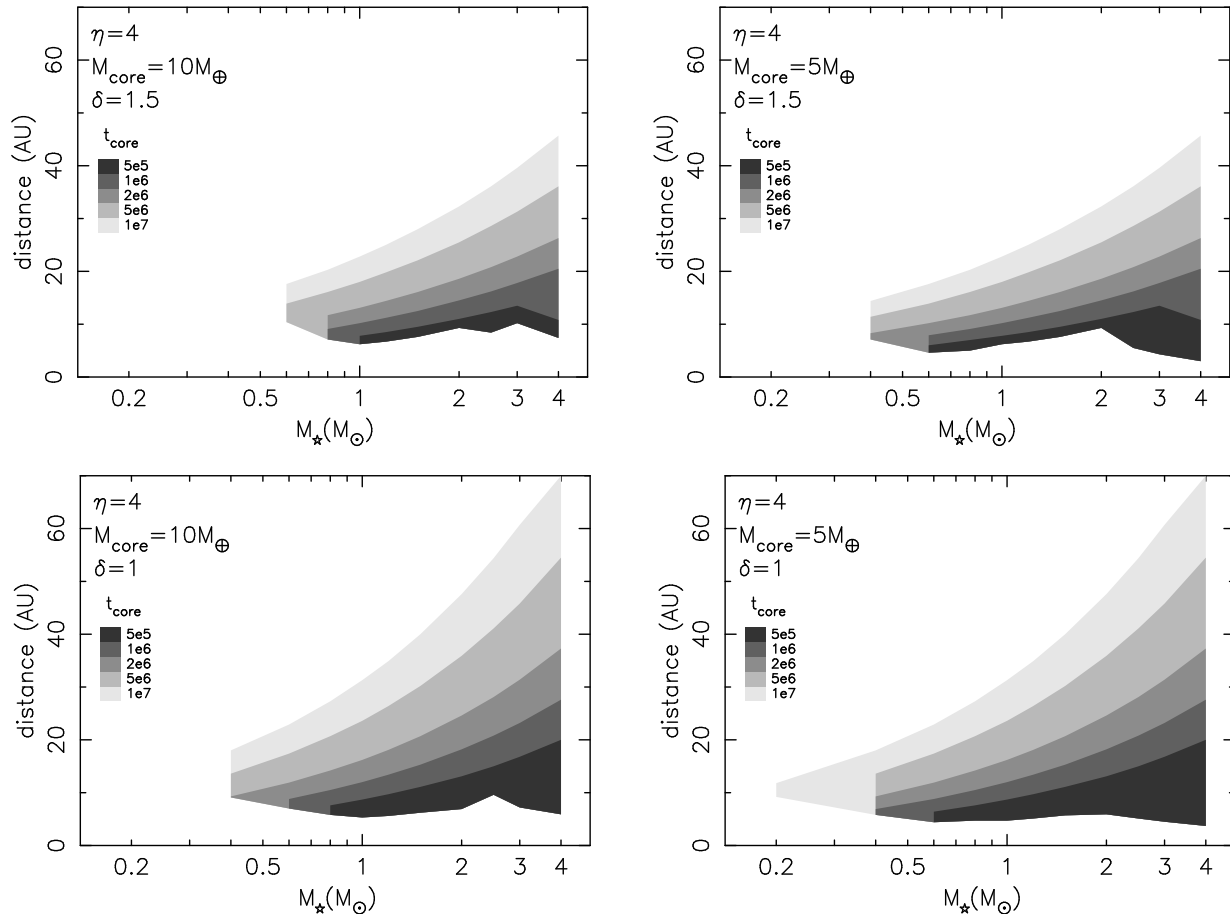


FIG. 6.— Similar to Figure 4, but for fixed  $\eta = 4$ . Contours represent different  $t_{\text{core}}$  as indicated by legends. Top (bottom) panels are  $\delta = 1.5$  ( $\delta = 1$ ), and left (right) panels are  $M_{\text{core}} = 10 M_{\oplus}$  ( $M_{\text{core}} = 5 M_{\oplus}$ ).

studies indicate that for cores less massive than  $\sim 10 M_{\oplus}$  the timescale is longer (Masset et al. 2006), and may be reduced to a random walk due to magnetohydrodynamic turbulence (Nelson & Papaloizou 2004). For cores with masses  $\gg 10 M_{\oplus}$  (Fig. 3) in relatively massive disks around intermediate mass stars, core accretion will likely occur before isolation, while planetesimals are still being accreted (Rafikov 2006). The successful formation of a gas giant then depends on whether the planet can reach a gap-opening mass before migrating into the central star.

Once a planet opens a gap in the disk it has survived the type I migration regime, but its continued existence is not guaranteed. Depending on the disk viscosity and lifetime, the planet can still migrate onto the central star by type II migration.

In summary, the simplicity of our model means that reasonable changes in the input parameters change the results little. Future development of the model can include a more complete treatment of more complicated physical processes.

## 6. DISCUSSION

The age of direct planet detection is approaching (e.g. NICI Campaign on Gemini South), where discoveries will be pushed to larger semi-major axes. In addition, radial velocity surveys now extend over a wider range of stellar masses (e.g. Frink et al. 2002; Butler et al. 2006; Johnson et al. 2007a,b). Our goal is to develop a theory of planet formation that extends over the observa-

tional range to make testable predictions, and to develop greater insight into the processes that produce the observed diversity of planetary systems.

For planets orbiting giant stars, there is a downward shift in the planet-metallicity distribution by  $\sim 0.3$  dex (Pasquini et al. 2007). This result is not surprising in the context of our model. In Figure 4, the lowest relative disk mass that forms cores roughly halves from 1 to  $2 M_{\odot}$ , which corresponds to a  $-0.3$  dex change in metallicity. Thus, we naturally expect the lower end of the metallicity distribution of higher mass stars to be shifted. However, we do not expect the high metallicity end of the distribution to move, since these disks can still form cores.

There are now sufficient planet discoveries to start quantifying trends across a range of stellar masses, which allows the first steps towards comparison with planet formation theories that consider the mass of the central star (e.g. Ida & Lin 2005). Though sample numbers are small, studies of  $\gtrsim 1.3 M_{\odot}$  giants indicate that giant planet frequency increases with stellar mass in the range  $0.1\text{--}2 M_{\odot}$  (Johnson et al. 2007a). We now calculate what our model predicts for the probability of forming gas giants as a function of stellar mass.

### 6.1. Gas Giant Frequency and Stellar Mass

Assuming all stars are born with a distribution of disk masses, we can estimate the probability  $P_{GG}$  of a star forming at least one gas giant as a function of stellar

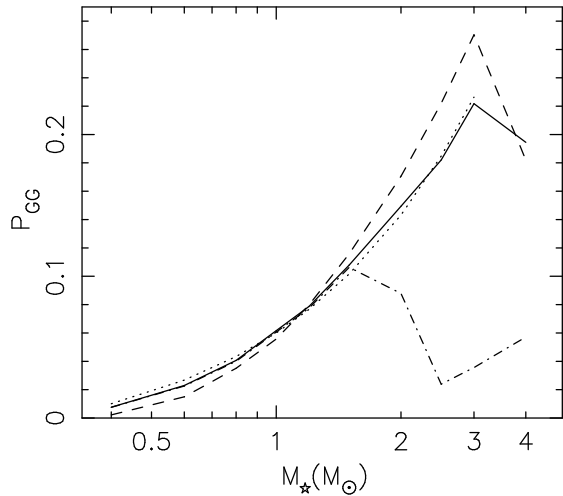


FIG. 7.— Probability of a star harbouring at least one gas giant planet as a function of stellar mass for our baseline model (solid line), and  $\delta = 1$  and  $M_{core} = 5 M_{\oplus}$  (dashed line). The thin dotted line is a fitted line of constant slope  $P_{M_{\star}} = 0.20 M_{\star} - 0.06$ . The dot-dashed line has  $a_{snow} \propto 2.7 M_{\star}^2$  AU, for comparison with Ida & Lin (2005). All curves are normalised to 6% at  $1 M_{\odot}$  via a straight line fit.

mass. Though comparison with observed disk masses is uncertain, we follow Ida & Lin (2005) and adopt a Gaussian distribution in terms of  $x = \log M_{disk}/M_{\star}$ , where  $P_{disk} \propto \exp\left(-\frac{(x - \mu)^2}{2\sigma_{ln}^2}\right)$  with standard deviation  $\sigma_{ln} = 1/3$ , centered on  $M_{disk} = 0.03 M_{\star}$  (e.g.  $\mu \approx -1.5$ ). This distribution is similar to data compiled by Natta et al. (2000), which is sensitive to all disk masses that form a core in our baseline model. Because our model is based on parameters that change with stellar mass (such as isolation time and disk mass), the relative probability of forming gas giants is our main concern. Effects that may set the absolute probability, such as survival of migrating planets, are not included. To make contact with observations, we therefore normalise our results to 6% for Solar-mass stars (Udry et al. 2007).

Figure 7 shows the likelihood of a star harbouring at least one gas giant planet as a function of stellar mass for our baseline model (Fig.4) and a model with  $\delta = 1$  and  $M_{core} = 5 M_{\oplus}$  (Fig.5), normalised to 6% at  $1 M_{\odot}$ . To illustrate the difference between a static, main-sequence scaled snow line, and our evolving one, we include a model with  $a_{snow} \propto 2.7 M_{\star}^2$  AU, similar to the main model of Ida & Lin (2005). Each point is the probability a star has a disk in the range that forms cores in Figure 4. This plot assumes that if one or more cores form, at least one will result in a gas giant. For comparison to current observations, it also assumes that as they accrete gas, cores generally migrate or scatter a stellar-mass independent fraction to observable distances, where the 6% normalisation applies. Like our baseline model, different  $M_{core}$ ,  $t_{core}$ , and  $\delta$  have lines of approximately constant slope ( $P_{GG} = m M_{\star} - c$ ) up to  $\sim 3 M_{\odot}$ . Our baseline model has  $m = 0.20$  and  $c = 0.06$ ; very few gas giants form by core accretion below  $0.3 M_{\odot}$ .

With the normalisation, our baseline model predicts 1% of  $0.4 M_{\odot}$  stars, and 10% of  $1.5 M_{\odot}$  stars will harbour at least one gas giant. Increasing  $\sigma_{ln}$  decreases the range of probabilities, because disk masses come from a less strongly varying section of the overall distribution.

For example,  $\sigma_{ln} = 1$  yields 4% and 8% for  $0.4 M_{\odot}$  and  $1.5 M_{\odot}$  stars respectively.

Our result is robust to changes in our assumed model parameters (in the range  $0.4$ – $1.5 M_{\odot}$ ), because the range of core forming disk masses generally remains the same, and the 6% normalisation removes absolute differences for different model parameters.

Despite its simplicity, our model modified to have a constant snow line at  $a_{snow} = 2.7 (M_{\star}/M_{\odot})^2$  AU produces a similar result to Ida & Lin (2005): that less gas giants form above a Solar mass. The difference arises from the stronger dependence of snow line distance with stellar mass. For stars  $\lesssim 3 M_{\odot}$  in our model, accretion largely determines the snow line distance, which suggests a better scaling is  $a_{snow} \propto M_{\star}^{4/9} \sigma_0^{2/9}$  if  $\dot{M} \propto \sigma_0$  and  $\sigma_g \propto M_{\star} a^{-3/2}$ . Alternatively,  $a_{snow} \propto M_{\star}^{6/9}$  if  $\dot{M} \propto M_{\star}$ , or  $a_{snow} \propto M_{\star}^{8/9}$  if  $\dot{M} \propto M_{\star}^2$ .

Finally, our probability calculation does not take the increasing core-forming region width with increasing stellar mass into account. Cores that form later at larger distances may be less susceptible to migrating into the central star, and stars with multiple planets may be more likely to retain at least one during migration and scattering processes. These effects have the potential to increase the frequency of giant planets as stellar mass increases.

## 7. SUMMARY AND CONCLUSIONS

We describe a model for the evolution of the snow line in a planet forming disk, and apply it over a range of stellar masses to derive the probability distribution of gas giants as a function of stellar mass. The two main ingredients for our model are a prescription for movement of the snow line due to accretion and PMS evolution, and rules that determine whether protoplanets are massive enough, and form early enough, to become gas giants.

The snow line distance generally moves inward over time. With our prescription for the accretion rate, accretion dominates over irradiation for stars with  $M_{\star} \lesssim 2 M_{\odot}$ . For  $\gtrsim 3 M_{\odot}$  stars, irradiation dominates at times  $\gtrsim 1$  Myr as the star moves up to its main-sequence luminosity. The transition is at a few Myr for  $\sim 2 M_{\odot}$  stars. Over the wide range of observed accretion rates for any fixed stellar mass, the snow line in some disks may be set entirely by irradiation.

The snow line generally sets where the innermost gas giant cores form. In relatively massive disks around intermediate mass stars, rocky cores form interior to the snow line. The location of the outermost core is always set by the gas dissipation timescale. The range of disk masses that form cores, and the radial width of the region in the disk where they form, increase with stellar mass. Lower mass disks produce failed icy cores, which are probably similar to Uranus, Neptune, and the observed “super-Earths.”

The outward movement of the snow line as stars more massive than the Sun reach the main-sequence, and as the disk becomes optically thin, allows the ocean planets suggested by Léger et al. (2004) to form *in situ*. The change in disk temperature is only large enough for these planets to harbour oceans around stars  $\gtrsim 2.5 M_{\odot}$ .

Our model includes several poorly determined parameters, which current and future facilities will investigate. While there are current resolved studies of gaseous disks

(e.g. Bitner et al. 2007), the next generation of telescopes such as GMT and ALMA will provide more information on surface density profiles, and how disk properties change with stellar mass and age. These studies will help to constrain input parameters for our model. We have shown that the time dependence of the snow line in part determines where gas giant cores form. This result should motivate future studies of planet formation in disks whose properties change with time.

The subsequent evolution of isolated cores is beyond the scope of this paper, but further work that investigates the growth and dynamical evolution of these objects can investigate the diversity of resulting system structures.

Given an initial distribution of disk masses, the probability that a star has at least one gas giant increases linearly with stellar mass from  $0.4 M_{\odot}$  to  $3 M_{\odot}$ . If the frequency of gas giants around solar-mass stars is 6%, we predict an occurrence rate of 1% (10%) for  $0.4 M_{\odot}$  ( $1.5 M_{\odot}$ ) stars. This result is largely insensitive to changes in our model parameters.

In contrast to the Ida & Lin (2005) model, where it is hard to form observable gas giants above  $1 M_{\odot}$ , our model predicts a peak at  $\sim 3 M_{\odot}$  because we include disk

and PMS evolution in our snow line derivation. However, our model does not include migration, so our prediction applies to observable and currently undetectable gas giants.

Though sample numbers are small, it appears that observable gas giant frequency increases with stellar mass across a wide range of host masses (Johnson et al. 2007a). Larger samples of stars that host giant planets, particularly low and intermediate-mass stars, will solidify this result. These studies, and the extension of the results to a wider range of semi-major axes, will provide a basis for comparison with our model predictions.

We acknowledge support from an Australian Post-graduate Award, a Smithsonian Astrophysical Observatory pre-doctoral fellowship (GK), and the *NASA Astrophysics Theory Program* through grants NAG5-13278 and NNG06GH25G (SK). We thank T. Currie, J. Johnson and the ANU Planetary Science Institute planet group for helpful discussions. We thank the anonymous referee for comments that improved the manuscript.

## REFERENCES

- Adams, F. C., Hollenbach, D., Laughlin, G., & Gorti, U. 2004, *ApJ*, 611, 360
- Adams, F. C. & Shu, F. H. 1986, *ApJ*, 308, 836
- Alexander, R. D., Clarke, C. J., & Pringle, J. E. 2006, *MNRAS*, 369, 229
- Andrews, S. M. & Williams, J. P. 2005, *ApJ*, 631, 1134
- Asplund, M., Grevesse, N., & Sauval, A. J. 2005, in *Astronomical Society of the Pacific Conference Series*, Vol. 336, *Cosmic Abundances as Records of Stellar Evolution and Nucleosynthesis*, ed. T. G. Barnes, III & F. N. Bash, 25–+
- Bell, K. R. & Lin, D. N. C. 1994, *ApJ*, 427, 987
- Bitner, M. A., Richter, M. J., Lacy, J. H., Greathouse, T. K., Jaffe, D. T., & Blake, G. A. 2007, *ArXiv e-prints*, 704
- Boss, A. P. 2006, *ApJ*, 643, 501
- Butler, R. P., Johnson, J. A., Marcy, G. W., Wright, J. T., Vogt, S. S., & Fischer, D. A. 2006, *PASP*, 118, 1685
- Chambers, J. E. 2006, *ApJ*, 652, L133
- Chiang, E. I. & Goldreich, P. 1997, *ApJ*, 490, 368
- Ciesla, F. J. & Cuzzi, J. N. 2006, *Icarus*, 181, 178
- Clarke, C. J., Gendrin, A., & Sotomayor, M. 2001, *MNRAS*, 328, 485
- Currie, T., Balog, Z., Kenyon, S. J., Rieke, G., Prato, L., Young, E. T., Muzerolle, J., Clemens, D. P., Buie, M., Sarcia, D., Grabu, A., Tollestrup, E. V., Taylor, B., Dunham, E., & Mace, G. 2007, *ApJ*, 659, 599
- Cuzzi, J. N. & Zahnle, K. J. 2004, *ApJ*, 614, 490
- Dullemond, C. P. & Dominik, C. 2005, *A&A*, 434, 971
- Eisner, J. A. & Carpenter, J. M. 2006, *ApJ*, 641, 1162
- Ford, E. B. & Chiang, E. I. 2007, *ApJ*, 661, 602
- Frink, S., Mitchell, D. S., Quirrenbach, A., Fischer, D. A., Marcy, G. W., & Butler, R. P. 2002, *ApJ*, 576, 478
- Garaud, P. & Lin, D. N. C. 2007, *ApJ*, 654, 606
- Goldreich, P., Lithwick, Y., & Sari, R. 2004, *ApJ*, 614, 497
- Greaves, J. S. et al. 2005, *ApJ*, 619, L187
- Haisch, Jr., K. E., Lada, E. A., & Lada, C. J. 2001a, *AJ*, 121, 2065
- 2001b, *ApJ*, 553, L153
- Hartmann, L., Calvet, N., Gullbring, E., & D'Alessio, P. 1998, *ApJ*, 495, 385
- Hayashi, C. 1981, *Progress of Theoretical Physics Supplement*, 70, 35
- Hollenbach, D. J., Yorke, H. W., & Johnstone, D. 2000, *Protostars and Planets IV*, 401
- Hubeny, I. 1990, *ApJ*, 351, 632
- Hubickyj, O., Bodenheimer, P., & Lissauer, J. J. 2005, *Icarus*, 179, 415
- Ida, S. & Lin, D. N. C. 2005, *ApJ*, 626, 1045
- Ikoma, M., Nakazawa, K., & Emori, H. 2000, *ApJ*, 537, 1013
- Inaba, S. & Ikoma, M. 2003, *A&A*, 410, 711
- Inaba, S., Wetherill, G. W., & Ikoma, M. 2003, *Icarus*, 166, 46
- Johnson, J. A., Butler, R. P., Marcy, G. W., Fischer, D. A., Vogt, S. S., Wright, J. T., & Peek, K. M. G. 2007a, *ArXiv e-prints*, 707
- Johnson, J. A., Fischer, D. A., Marcy, G. W., Wright, J. T., Driscoll, P., Butler, R. P., Hekker, S., Reffert, S., & Vogt, S. S. 2007b, *ArXiv e-prints*, 704
- Kasting, J. F., Whitmire, D. P., & Reynolds, R. T. 1993, *Icarus*, 101, 108
- Kennedy, G. M., Kenyon, S. J., & Bromley, B. C. 2006, *ApJ*, 650, L139
- Kenyon, S. J. & Bromley, B. C. 2004a, *AJ*, 127, 513
- 2004b, *ApJ*, 602, L133
- Kenyon, S. J. & Hartmann, L. 1987, *ApJ*, 323, 714
- 1995, *ApJS*, 101, 117
- Kokubo, E. & Ida, S. 1996, *Icarus*, 123, 180
- 1998, *Icarus*, 131, 171
- Kornet, K., Wolf, S., & Różycka, M. 2006, *A&A*, 458, 661
- Küppers, M. et al. 2005, *Nature*, 437, 987
- Laughlin, G., Bodenheimer, P., & Adams, F. C. 2004, *ApJ*, 612, L73
- Lecar, M., Podolak, M., Sasselov, D., & Chiang, E. 2006, *ApJ*, 640, 1115
- Léger, A., Selsis, F., Sotin, C., Guillot, T., Despois, D., Mawet, D., Ollivier, M., Labèque, A., Valette, C., Brachet, F., Chazelas, B., & Lammer, H. 2004, *Icarus*, 169, 499
- Lin, D. N. C. & Papaloizou, J. 1985, in *Protostars and Planets II*, ed. D. C. Black & M. S. Matthews, 981–1072
- Lissauer, J. J. 1987, *Icarus*, 69, 249
- Lissauer, J. J. & Stevenson, D. J. 2007, in *Protostars and Planets V*, ed. B. Reipurth, D. Jewitt, & K. Keil, 591–606
- Lynden-Bell, D. & Pringle, J. E. 1974, *MNRAS*, 168, 603
- Masset, F. S., D'Angelo, G., & Kley, W. 2006, *ApJ*, 652, 730
- McCaughrean, M. J. & O'dell, C. R. 1996, *AJ*, 111, 1977
- Muzerolle, J., Hillenbrand, L., Calvet, N., Briceño, C., & Hartmann, L. 2003, *ApJ*, 592, 266
- Nakano, T. 1987, *MNRAS*, 224, 107
- 1988a, *MNRAS*, 230, 551
- 1988b, *MNRAS*, 235, 193
- Natta, A., Grinin, V., & Mannings, V. 2000, *Protostars and Planets IV*, 559
- Nelson, R. P. & Papaloizou, J. C. B. 2004, *MNRAS*, 350, 849
- Osterloh, M. & Beckwith, S. V. W. 1995, *ApJ*, 439, 288

- Palla, F. & Stahler, S. W. 1999, *ApJ*, 525, 772
- Pascucci, I. et al. 2006, *ApJ*, 651, 1177
- Pasquini, L., Doellinger, M. P., Weiss, A., Girardi, L., Chavero, C., Hatzes, A. P., da Silva, L., & Setiawan, J. 2007, *ArXiv e-prints*, 707
- Podolak, M. & Zucker, S. 2004, *Meteoritics and Planetary Science*, 39, 1859
- Pollack, J. B., Hubickyj, O., Bodenheimer, P., Lissauer, J. J., Podolak, M., & Greenzweig, Y. 1996, *Icarus*, 124, 62
- Rafikov, R. R. 2004, *AJ*, 128, 1348
- . 2006, *ApJ*, 648, 666
- Rieke, G. H., Su, K. Y. L., Stansberry, J. A., Trilling, D., Bryden, G., Muzerolle, J., White, B., Gorlova, N., Young, E. T., Beichman, C. A., Stapelfeldt, K. R., & Hines, D. C. 2005, *ApJ*, 620, 1010
- Rivera, E. J., Lissauer, J. J., Butler, R. P., Marcy, G. W., Vogt, S. S., Fischer, D. A., Brown, T. M., Laughlin, G., & Henry, G. W. 2005, *ApJ*, 634, 625
- Safronov, V. S. 1969, *Evolution of the Protoplanetary Cloud and Formation of the Earth and Planets* (Moscow: Nauka; English transl. 1972 [NASA TT F-677])
- Sasselov, D. D. & Lecar, M. 2000, *ApJ*, 528, 995
- Saumon, D. & Guillot, T. 2004, *ApJ*, 609, 1170
- Scholz, A., Jayawardhana, R., & Wood, K. 2006, *ApJ*, 645, 1498
- Strom, S. E., Edwards, S., & Skrutskie, M. F. 1993, in *Protostars and Planets III*, ed. E. H. Levy & J. I. Lunine, 837–866
- Tanaka, H., Takeuchi, T., & Ward, W. R. 2002, *ApJ*, 565, 1257
- Thommes, E. W., Duncan, M. J., & Levison, H. F. 1999, *Nature*, 402, 635
- Udry, S., Fischer, D., & Queloz, D. 2007, in *Protostars and Planets V*, ed. B. Reipurth, D. Jewitt, & K. Keil, 685–699
- Weidenschilling, S. J. 1977, *Ap&SS*, 51, 153
- . 2000, *Space Science Reviews*, 92, 295
- Wetherill, G. W. & Stewart, G. R. 1989, *Icarus*, 77, 330
- Zuckerman, B., Forveille, T., & Kastner, J. H. 1995, *Nature*, 373, 494